

# Microturbulence Study of the Isotope Effect

A. Bustos,<sup>1</sup> A. Bañón Navarro,<sup>1</sup> T. Görler,<sup>1</sup> F. Jenko,<sup>1,2,3</sup> and C. Hidalgo<sup>4</sup>

<sup>1</sup>Max-Planck-Institut für Plasmaphysik, Boltzmannstrasse 2, 85748 Garching, Germany

<sup>2</sup>Max-Planck/Princeton Center for Plasma Physics

<sup>3</sup>Department of Physics and Astronomy, University of California, Los Angeles, California 90095, USA

<sup>4</sup>Laboratorio Nacional de Fusion, CIEMAT, 28040 Madrid, Spain

The influence of the ion mass on the dynamics of magnetized plasmas is an important challenge in fusion research. The discrepancies between the improvement of the magnetic confinement with the ion mass in tokamak experiments and diffusive turbulent transport predictions have remained unexplained for several decades. We refer to this phenomenon as the *isotope effect*. In this paper we study this effect with gyrokinetic theory using the GENE code. We find several sets of plasma parameters that correspond to low wavenumber turbulence for which the isotope effect is present, although the intensity is smaller than the experimental observations. We also relate these results to the zonal flow intensity of the system, which is characterized by the average shear flow rate.

## I. INTRODUCTION

It has been observed in many tokamak experiments that the plasma confinement properties improve with increasing atomic mass of the hydrogen isotope used (H, D, T). On the other hand, standard gyro-Bohm theory predicts a square root scaling of the turbulent diffusivities with the ion mass, with the consequent deterioration of the confinement. This disagreement between experiments and theoretical predictions is presently unexplained, and it is usually called the *isotope effect*.

Many experiments have been done to study the scaling of the confinement with the isotope mass for different plasma conditions and heating regimes. In the ASDEX Upgrade tokamak the confinement was improved up to 100% with deuterium H-mode discharges compared to hydrogen discharges.<sup>1–3</sup> In addition, experiments in TFTR measured improvement in the confinement if tritium is added to deuterium plasmas.<sup>4</sup> The influence of ion mass on confinement seems to be weaker in stellarators<sup>5</sup> with ongoing experimental studies to investigate the role of plasma collisionality.<sup>6</sup>

The isotope effect could have strong influence on the power threshold of the L-H transition in tokamaks, with direct impact on future D-T operation.<sup>7</sup> As an example, assuming the experimental scaling with the mass, the power threshold for hydrogen plasmas in ITER is expected to be reduced around 50% when using deuterium instead of hydrogen. On the contrary, if the power threshold satisfies gyro-Bohm scaling, the H-mode in ITER will be very difficult to achieve. Consequently, the understanding of this effect is important for the design and performance of future fusion devices.

In spite of the experimental observations, there is no complete theoretical or numerical description of this phenomenon. In recent TEXTOR experiments,<sup>8</sup> it has been measured that the correlation length in the poloidal direction of the electric potential increases with the effective mass in H/D plasmas. Thus, it is likely that the zonal flows became stronger and the turbulence was reduced. Hahn *et al.*<sup>9</sup> suggest that trapped electron mode (TEM) turbulence is influenced by the isotope mass. Linear analytical calculations show that the residual level of zonal flows is higher for D than for H, pointing to a possible improvement of the confinement.

Based on these previous works, we report ITG (ion temperature gradient) and TEM simulations performed with the GENE code for the three hydrogen isotopes. We emphasize the study of the effects of zonal flows on the transport regulation. In order to simplify the problem, we choose a simple circular geometry as well as Cyclone-Base-Case (CBC) parameters<sup>10</sup> and do not consider collisions and finite- $\beta$  effects.

The layout of this paper is organized as follows: in Sec. II we briefly describe the GENE code and in Secs. III and IV we show the linear and nonlinear simulation results for ITG and TEM. Finally we present the conclusions in Sec. V.

## II. THE GENE CODE

The GENE (Gyrokinetic Electromagnetic Numerical Experiment) code<sup>11</sup> solves the gyrokinetic equations<sup>12</sup> using an Eulerian  $\delta f$  approach. It integrates the nonlinear gyrokinetic equation using a fixed grid in the 5D phase space. GENE includes many physical effects: an arbitrary number of kinetic species, electromagnetic fluctuations, collision operator (Landau-Boltzmann) with momentum conservation and a neoclassical solver. The code can use realistic geometries via interfaces with equilibrium codes like VMEC or EFIT. It has been extensively benchmarked with other codes and experiments and optimized, showing a good scaling up to more than  $10^5$  cores. More details can be found in the code web page.<sup>13</sup>

GENE uses a system of field-aligned coordinates  $(x, y, z, v_{\parallel}, \mu)$ . The  $z$  coordinate is parallel to the magnetic field. In the flux tube approximation used here, the background magnetic field depends only on  $z$ . The radial coordinate  $x$  determines the flux surface and the binormal coordinate  $y$  selects the magnetic field line. Since we use periodic boundary conditions for  $x$  and  $y$ , all quantities are transformed to Fourier space  $(k_x, k_y)$  in that dimensions. As usual,  $v_{\parallel}$  and  $\mu$  are the parallel component of the velocity and the magnetic moment, respectively.

We remark that in the local approximation considered, no global (finite  $\rho^* = \rho_i/a$ ) effects are taken into account. Thus, our results are caused by the mass difference between species. Also no neoclassical effects (either the neoclassical source

term in the gyrokinetic equation or the long wavelength radial electric field) are included.

In the simulations presented here, we use a well known technique in fluid computations applied to gyrokinetics: Gyrokinetic Large Eddy Simulations (GLES).<sup>14,15</sup> This numerical technique dynamically adjusts the spatial perpendicular hyperdiffusions of the simulation. In this way we are able to reduce the number of nodes in the perpendicular directions ( $N_x$  and  $N_y$ ) and to speed up GENE simulations a factor of 10-20 in some cases.

### III. LINEAR SIMULATIONS

The geometry used both in linear and nonlinear simulations is a circular tokamak with concentric flux surfaces and CBC parameters: major radius  $R_0 = 1.65$  m, magnetic field at the axis  $B_0 = 1$  T, safety factor  $q = 1.4$ ,  $\epsilon = r/R_0 = 0.18$  and magnetic shear  $\hat{s} = \frac{r}{q} \frac{dq}{dr} = 0.8$ . The plasma density is  $n = 3.5 \cdot 10^{19} \text{ m}^{-3}$  and, unless otherwise specified, the ion and electron temperatures are  $T_i = T_e = 0.35$  keV. In this section we study the Rosenbluth-Hinton residual level of zonal flows and the linear growth rates of the instabilities.

#### A. Rosenbluth-Hinton Test

Rosenbluth-Hinton (RH) tests<sup>16</sup> are linear simulations that show the residual values of the zonal flows in our system. There are several numerical techniques to calculate this value, all related to the collisionless damping of zonal flows.

In GENE we choose to impose an external and static zonal flow  $\Phi_{\text{ext}}(k_x)$  for some finite  $k_x$ , being all other components equal to zero. The perturbed distribution function  $\delta f$  evolves starting from  $\delta f(t=0) = 0$ . Then the system responds creating a potential  $\Phi_1(k_x, t)$ , but the total  $\Phi = \Phi_{\text{ext}} + \Phi_1$  is not fully damped at large times. We measure the normalized residual level, defined as:

$$\text{R.H. residual level} = \frac{\Phi(k_x, t \rightarrow \infty)}{\Phi(k_x, t=0)} = \frac{[\Phi_{\text{ext}} + \Phi_1](k_x, t \rightarrow \infty)}{\Phi_{\text{ext}}(k_x, t=0)}. \quad (1)$$

FIG. 1 shows the RH residual value for the three isotopes considered: hydrogen, deuterium and tritium.

The parameter  $\tau = T_e/T_i$  plays a key role in TEM<sup>17,18</sup> turbulence. Thus we study the cases with  $\tau = 1$  and  $\tau = 3$ . GENE is able to reproduce the analytical predictions of Hahn<sup>9</sup> for  $\tau = 1$ : at scales  $0.001 \lesssim k_x \rho_e \lesssim 0.1$ , the residual zonal flow level increases with the isotope mass. If the confinement properties of the system depend on the RH residual level, they will be different for each ion species. The isotope effect could then be visible in the range  $0.001 \lesssim k_x \rho_e \lesssim 0.1$ , or  $0.05 \lesssim k_x \rho_i \lesssim 5$ , which corresponds to ITG and TEM turbulence.<sup>19</sup> The resilience of the zonal flows in the system is different for  $\tau = 1$  and for  $\tau = 3$ . There is isotopic dependence also for  $\tau = 3$ , but at smaller levels than those for  $\tau = 1$ . This suggests that zonal flows may be weaker for  $\tau = 3$  than for

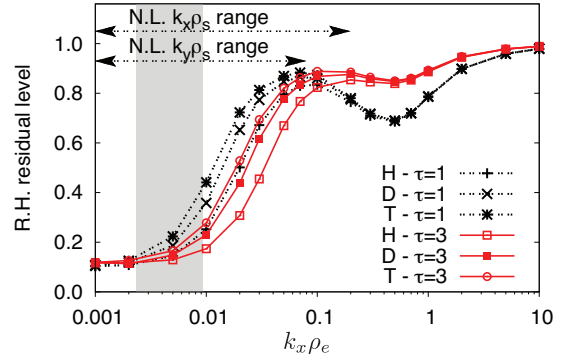


FIG. 1: Rosenbluth-Hinton test for H,D,T for the cases  $\tau = 1$  (black lines) and  $\tau = 3$  (red lines). The black arrows indicate the  $k_x \rho_s$  and  $k_y \rho_s$  range in the nonlinear simulations performed. The shaded area indicates the approximate  $k_x$  interval in which the flux spectra peak.

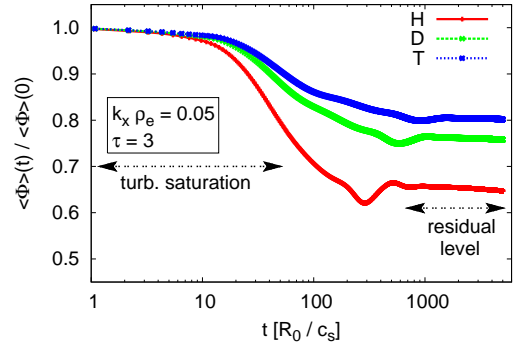


FIG. 2: Zonal flow time trace. The approximate turbulence saturation time and time interval for the residual level calculation are indicated in the plot.

$\tau = 1$ , and may be related to the relation of thermal velocities of the species:  $\frac{v_{\text{th},i}}{v_{\text{th},e}} \sim \sqrt{\frac{m_e}{m_i}} \frac{1}{\sqrt{\tau}}$ . This is supported by the results of FIG. 1, where the quotient is equal for (H,  $\tau = 3$ ) and (T,  $\tau = 1$ ) and the R.H. residual level is almost the same at ion scales.

Not only the zonal flow residual level is important to regulate the turbulence, but also the isotopic dependence during the typical saturation time. We have checked that this time is roughly  $\tau_{\text{turb}} \sim 50 [R_0 / c_s]$ . FIG. 2 displays the zonal flow time trace at a spatial scale in which isotopic dependence of the residual level is present. The zonal flow exhibits isotopic dependence during  $\tau_{\text{turb}}$ , pointing out that the nonlinear phase can be affected.

#### B. Linear ITG Simulations

We perform linear ITG simulations for the three hydrogen isotopes to study the linear phase of the turbulence. We calculate the growth rate of the most unstable mode as a function of the wavenumber in the  $y$  direction ( $k_y$ ). ITG growth rates

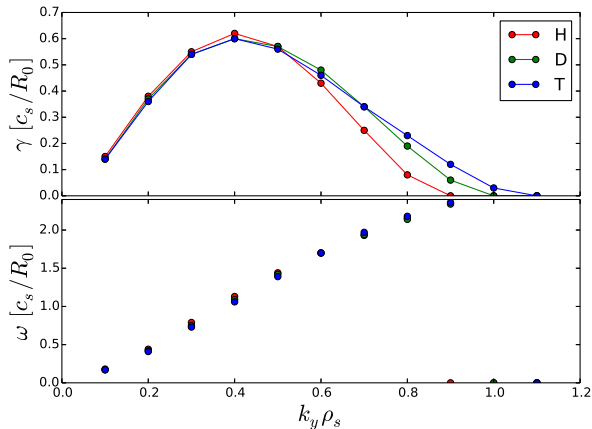


FIG. 3: ITG linear growth rates and frequencies with kinetic electrons, using  $\omega_{Ti} = 6.9$ ,  $\omega_n = 2.2$ ,  $\omega_{Te} = 0.0$ .  $R_0$  is the major radius of the tokamak and  $c_s$  and  $\rho_s$  are the isotope sound speed and gyroradius, respectively, which depend on the ion mass.

peak in the range  $k_y \rho_i = 0.1 - 1$ , being  $\rho_i$  the ion gyroradius. This is a range in which the RH tests predict isotopic dependence of the zonal flows.

The plasma parameters used are those from the CBC case, with normalized gradients of  $\omega_{Ti} = -\frac{R_0}{T_i} \frac{dT_i}{dr} = 6.9$ ,  $\omega_{Te} = 0$  and  $\omega_n = -\frac{R_0}{n} \frac{dn}{dr} = 2.2$ . We find an isotopic dependence in the growth rates, as can be seen in FIG. 3, for  $k_y \rho_s \geq 0.5$ . This feature, combined with the residual flow level may introduce an isotopic dependence in the nonlinear regime.

### C. Linear TEM Simulations

TEM turbulence can be driven by electron temperature gradients ( $\omega_{Te}$ ) or by density gradients ( $\omega_n$ ). They produce particle and heat transport and require kinetic electrons. TEMs exist on similar scales as ITGs, peaking around  $k_y \rho_i \sim 1$ . In order to isolate the TEMs, we set the ion temperature gradient to zero:  $\omega_{Ti} = 0$ . We fix  $\omega_n$  equal to 6 and 3 and scan over the electron temperature gradient  $\omega_{Te}$  to study different types of turbulence. It is known that, depending on the values of  $\omega_{Te}$ ,  $\omega_n$  and  $\tau = T_e/T_i$ , the zonal flows have different influence in the physics of the system.<sup>18</sup>

The simulations introduce the mass dependence by decreasing the electron mass and keeping the ion mass constant. Thus, we increase the ion/electron mass ratio while keeping the ion sound gyroradius constant. Since TEMs peak in  $\rho_i \sim 1$ , this technique is more convenient from a computational point of view because all three isotopes share the same  $\rho_s$ . Then, to transform heat fluxes to the International System, one has to multiply by the square root of the atomic mass  $\sqrt{A}$ .

In order to assure that we are dealing with TEM modes, we plot in FIGs. 4 and 5 the most unstable mode for  $\omega_n = 6$ ,  $\omega_{Te} = 12$ , varying  $\tau$ . Based on previous gyrokinetic mul-

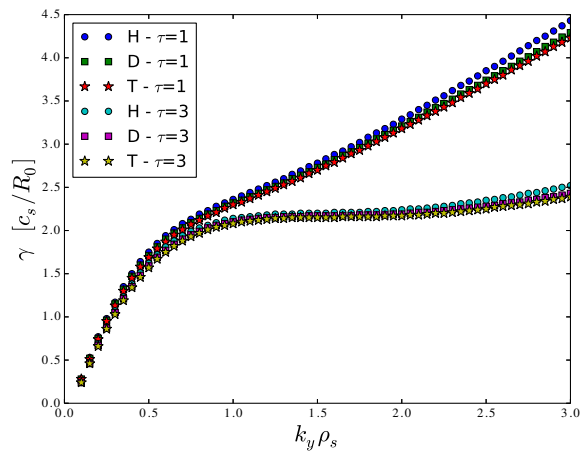


FIG. 4: Suppression of the ETG instability by increasing the electron/ion temperature ratio  $\tau$  for  $\omega_n = 6$  and  $\omega_{Te} = 12$ . TEMs develop in the region of  $k_y \rho_s \lesssim 1$ , and the influence of ETG for  $k_y \rho_s \leq 3$  is very weak. Note that  $\gamma$  units depend on  $c_s$ , which is proportional to  $A^{-1/2}$ .

tiscale simulations with GENE, it is reasonable to expect that pronounced contributions from ETG turbulence tend to be correlated with  $\frac{\gamma_{ETG}}{\gamma_{ITG/TEM}} \gtrsim \sqrt{\frac{m_i}{m_e}}$ .<sup>20</sup> It is also known<sup>21</sup> that increasing  $\tau$  suppresses the ETG. FIG. 4 shows the low  $k_y$  part of the spectrum where TEM develops. For a given  $\tau$ , the small differences in the growth rate spectra are due to the influence of the ETG modes. The growth rate spectra are plotted up to electron scales in FIG. 5. ETG modes develop around  $k_y \rho_e \sim 1$  or  $k_y \rho_s \sim 50$ , and most of the isotopic dependence is located at  $k_y \rho_s \geq 10$ . With these amplitudes of the low and high growth rate spectra, with quotients of the order of  $\frac{\gamma_{ETG}}{\gamma_{ITG/TEM}} \lesssim (15, 20, 30)$  for (H,D,T), we assume that the ETG contribution to the transport is negligible. In order to resolve TEM or ITG turbulence we restrict to  $k_y \rho_s \leq 3.2$ . In this wavelength range considered, the isotope mass does not affect the linear growth rates. Additionally, the use of the GLES technique reduces the turbulence activity in the smallest scales (see the flux spectra in Sec. IV A).

### IV. NONLINEAR SIMULATIONS

In nonlinear simulations new physical phenomena arise. This include saturation mechanisms, in which zonal flows can play an important role. The aim of this section is to study the confinement of different turbulent systems, defined by their drive ( $\omega_{Ti}$ ,  $\omega_{Te}$ ,  $\omega_n$ ) and the electron/ion temperature ratio ( $\tau$ ), using H, D or T as the ion species.

We choose the outward heat or energy flux as the transport quantity to characterize the confinement. It is defined as:

$$Q = \sum_{\alpha} \langle \langle \int \frac{m_{\alpha} v^2}{2} (\mathbf{v}_{E \times B})^x T^* \delta f_{\alpha} d^3 \mathbf{v} \rangle \rangle_t, \quad (2)$$

where  $\alpha$  denotes the particle species,  $\langle \cdot \rangle$  is the flux surface

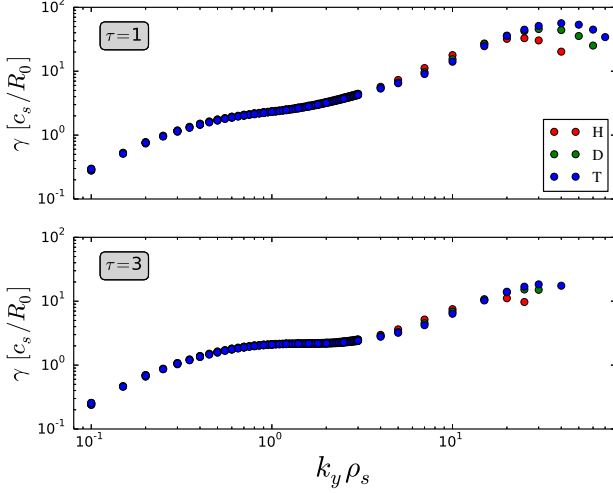


FIG. 5: TEM case - Linear growth rate spectrum for a wide  $k_y \rho_s$  range. ETGs peak in different scales because we introduce the isotope effect varying the electron mass in GENE. Since we are limited to  $k_y \rho_s \leq 3.2$ , the ETG influence on the simulation is negligible.

average and  $\langle \cdot \rangle_t$  is the time average.  $T^*$  is the so called *pull back* operator, which transforms  $\delta f_\alpha$  from gyrocenter to guiding center coordinates taking into account the gyrokinetic polarization terms<sup>12</sup>. Finally,  $(\mathbf{v}_{E \times B})^x$  is the radial component of the turbulent  $E \times B$  velocity:  $\mathbf{v}_{E \times B} = -\nabla \hat{\Phi} \times \mathbf{B} / B^2$ , where  $\hat{\Phi}(x, y, z)$  is the fluctuating electric potential.

If  $Q$  follows the gyro-Bohm scaling, then the relation of the heat fluxes of different isotopes of mass  $A$  is:

$$Q(A) = Q(A=1) \cdot \sqrt{A}. \quad (3)$$

We perform almost 50 nonlinear simulations for ITG and TEM turbulence, studying different systems with diverse zonal flow influence. Then we identify the cases that deviate from the gyro-Bohm predictions.

### A. Nonlinear ITG/TEM Simulations

We study the isotopic dependence in the nonlinear heat flux in a mixed set of ITG/TEM modes. Although in this case the turbulence is driven mainly by  $\omega_{Ti}$  and we set  $\omega_{Te} = 0$ , some TEM activity may appear since we have  $\omega_n \neq 0$ . For these simulations we use the following grid:  $N_x = 256$ ,  $N_y = 64$ ,  $N_z = 24$ ,  $N_v = 48$ ,  $N_\mu = 20$ . We neglect collisions and beta effects and limit to the range  $0 \leq k_y \rho_s \leq 3.2$ . Convergence studies have been performed to justify the results presented in this work. Thus, several non-physical parameters of the simulations have been checked for numerical convergence. We find that the most important parameter is the number of grid points in the radial direction ( $N_x$ ). In Fig. 6 we plot the nonlinear heat fluxes for the three hydrogen isotopes in a TEM scenario using  $N_x = 256, 512, 768$ . Since we are interested

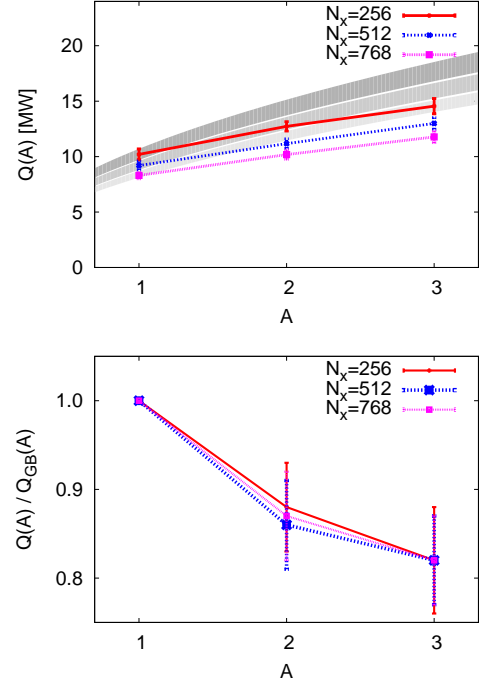


FIG. 6: Convergence studies for TEM turbulence with drive  $\omega_n = 6$ ,  $\omega_{Ti} = 0$  and  $\omega_{Te} = 12$ . In the upper plot we can see the absolute value of the nonlinear heat flux for H, D and T using three different grid sizes in the radial direction ( $N_x$ ). Shaded areas indicate the region in which the heat flux is compatible with gyro-Bohm scaling of  $Q(A=1)$  within its error bars. The lower plot shows the quotient of the nonlinear heat flux and the gyro-Bohm prediction, which does not depend on  $N_x$ .

in deviations from gyro-Bohm scaling, we plot the quotient  $Q(A)/Q_{GB}(A)$  in Fig. 6 (lower plot). We observe that this quotient is constant within the error bars for all  $N_x$  used. So, even in the absolute value of  $Q$  is not totally correct, a correct measurement of the deviation from Gyro-Bohm theory is obtained with  $N_x = 256$ . Consequently, we fix  $N_x = 256$  in order to minimize the computational cost.

We explore different physical scenarios, characterized by the turbulence drive ( $\omega$ 's) and plasma properties ( $\tau$ ). TABLE I summarizes the main parameters of the simulations, labeled as ITG/TEM. The fluxes corresponding to cases 1 to 3 are plotted in FIG. 7. We introduce a quantity to measure the relative deviation from the classical scaling of the time average heat flux. Let us assume we have two isotopes with masses  $m_a$  and  $m_b$  and the heat fluxes derived from GENE are  $Q_a$  and  $Q_b$ . Dividing the heat flux by the square root of the mass gives mass independent quantities that should be equal if gyro-Bohm scaling is satisfied. Then we define the relative deviation as:

$$\Delta_{ab} = \frac{Q_a / \sqrt{m_a} - Q_b / \sqrt{m_b}}{Q_a / \sqrt{m_a}}. \quad (4)$$

Its error is calculated using quadratic propagation of errors.

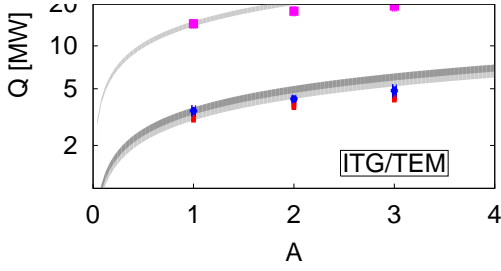


FIG. 7: Nonlinear heat fluxes for the ITG/TEM cases considered in TABLE I. Shaded areas indicate the region in which the heat flux is compatible with gyro-Bohm scaling of  $Q(A=1)$  within its error-bars.

Label	$\omega_{Ti}$	$\omega_{Te}$	$\omega_n$	$\Delta_{HT}$ (%)	$\Delta_{HD}$ (%)	$\Delta_{DT}$ (%)
ITG/TEM-1	6.9	0.0	2.2	$22 \pm 9$	$15 \pm 10$	$8 \pm 9$
ITG/TEM-2	6.9	6.0	2.2	$22 \pm 7$	$16 \pm 6$	$7 \pm 9$
ITG/TEM-3	6.9	12.0	6.0	$23 \pm 5$	$13 \pm 6$	$11 \pm 7$
Marginal	4.0	0.0	2.2	$21 \pm 8$	$21 \pm 11$	$0 \pm 13$

TABLE I: Main parameters of the ITG/TEM simulations and deviation from gyro-Bohm scaling.

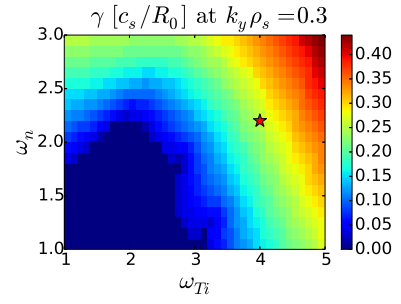
Table I shows that the deviation from gyro-Bohm scaling from H to T ( $\Delta_{HT}$ ) is approximately 20% in the cases studied. It can also be observed that there is more deviation when changing the isotope from H to D than from D to T:  $\Delta_{HD} > \Delta_{DT}$ .

A more physically relevant system is the ITG/TEM marginally unstable case. Marginally unstable means that the turbulence source ( $\omega_{Ti}, \omega_{Te}, \omega_n$ ) is outside but near the stable region, characterized by  $\gamma \leq 0$ . This case is supposed to be closer to an experimental plasma. In FIG. 8a we plot  $\gamma(\omega_{Ti}, \omega_n)$ , fixing  $\omega_{Te} = 0$ . Taking into account the nonlinear Dimits shift<sup>10</sup>, we choose  $\omega_n = 2.2$  and  $\omega_{Ti} = 4.0$  as our marginally unstable ITG/TEM. The nonlinear fluxes are depicted in FIG. 8b, showing similar isotope effect as ITG/TEMs 1 to 3.

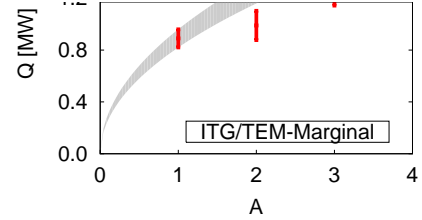
We have also checked the effect of GLES in a system with kinetic electrons. In FIG. 9 we plot the heat flux spectra as a function of the perpendicular wave vectors  $k_x$  and  $k_y$ . As expected, GLES do not affect the spectrum at large scales and do not change the total heat flux (compatible within error bars). GLES affect the decay of the heat flux at the high wavenumber region of the spectra, reducing the influence of high  $k$  turbulence (ETG) and avoiding the accumulation of energy.

## B. Nonlinear TEM Simulations

For TEM simulations we also need the grid with  $N_x = 256$ ,  $N_y = 64$ ,  $N_z = 24$ ,  $N_v = 48$  and  $N_\mu = 20$ . The perpendicular box dimensions are chosen to be  $l_x = 200\rho_s$  and



(a) Growth rate  $\gamma$  for H. The red star denotes the gradients chosen for the nonlinear run.



(b) Nonlinear heat fluxes for the marginally unstable ITG/TEM.

FIG. 8: Marginally unstable ITG/TEM results.

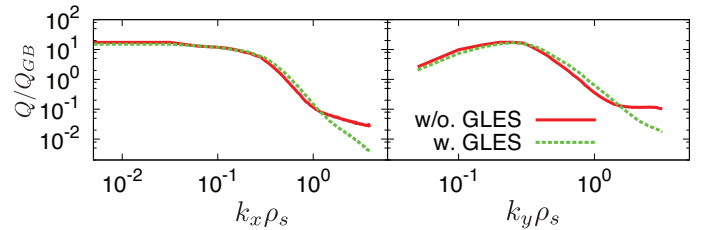


FIG. 9: Ion heat flux spectra, in gyro-Bohm units, as a function of the perpendicular wave vectors with and without Gyrokinetic Large Eddy Simulations [GLES]. The total time averaged fluxes are  $Q_{w./o.GLES} = 10.2 \pm 0.5$  MW and  $Q_{w./o.GLES} = 9.6 \pm 0.5$  MW.

$l_y = 125\rho_s$ . It is important to have a sufficiently large  $l_x$  in TEM simulations, because streamers of the electric potential can be very elongated in the  $x$  direction. We always keep  $\omega_{Ti} = 0$  to remove any ITG turbulence. TABLE II shows the main parameters of the simulation and the deviation from gyro-Bohm prediction in the nonlinear regime.

The nonlinear total heat flux is plotted in FIG. 10. For  $\omega_n = 6$  and  $\tau = 1$  we observe clear deviations from  $\sqrt{A}$  scaling, quantified in TABLE II. It is favorable for the confinement, although it is not as large as the experiments suggest. Its relative value is similar for those obtained in ITG/TEM turbulence. There is also a tendency to saturate with the mass, like in the simulations performed with GYRO.<sup>22</sup> The isotope effect disappears when we increase the temperature ratio to

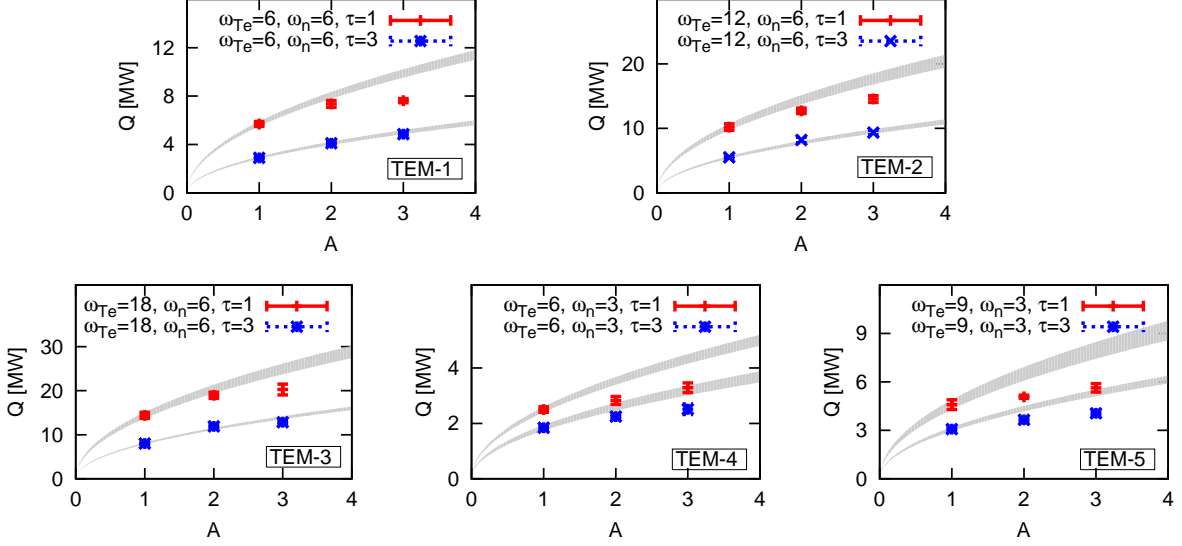


FIG. 10: Nonlinear radial heat flux as a function of the isotope mass for the different TEM turbulence cases considered. Shaded areas indicate the region in which the heat flux is compatible with gyro-Bohm scaling of  $Q(A=1)$  within its error bars.

$\tau = 3$  and  $Q(A)$  follows almost perfectly the  $\propto \sqrt{A}$  scaling. For  $\omega_n = 3$  (TEM-4 and TEM-5), the deviation is present in all cases studied. The quantity  $\Delta_{ab}$  presents more interesting features than in the pure ITG cases. For TEM-4 and TEM-5,

it behaves in a similar way because  $\Delta_{HD} > \Delta_{DT}$ . However, TEM-1-2-3 behave differently since  $\Delta_{HD} < \Delta_{DT}$  in most of the simulations.

Label	$\omega_{Te}$	$\omega_n$	$\tau$	$\Delta_{HT}$ (%)	$\Delta_{HD}$ (%)	$\Delta_{DT}$ (%)
TEM-1	6	6	1	$23 \pm 4$	$10 \pm 4$	$15 \pm 4$
	6	6	3	$5 \pm 5$	$1 \pm 5$	$4 \pm 5$
TEM-2	12	6	1	$18 \pm 5$	$14 \pm 5$	$6 \pm 5$
	12	6	3	$2 \pm 5$	$-6 \pm 7$	$7 \pm 6$
TEM-3	18	6	1	$18 \pm 6$	$7 \pm 6$	$13 \pm 6$
	18	6	3	$7 \pm 4$	$-4 \pm 5$	$11 \pm 5$
TEM-4	6	3	1	$21 \pm 5$	$24 \pm 4$	$3 \pm 5$
	6	3	3	$21 \pm 7$	$16 \pm 5$	$9 \pm 8$
TEM-5	9	3	1	$29 \pm 6$	$28 \pm 5$	$9 \pm 5$
	9	3	3	$24 \pm 4$	$19 \pm 4$	$9 \pm 5$

TABLE II: Main parameters of the TEM simulations and relative deviation of the heat flux from gyro-Bohm scaling.

### C. Zonal Flow Discussion

We can characterize the influence of the zonal flows in the system with the quotient of the average  $E \times B$  shear rate ( $\omega_{E \times B}$ ) and the maximum linear growth rate. This represents the ratio between the strength of the instability (growth rate) and the intensity of one of the lead saturation mechanisms. The shear rate is defined as  $\omega_{E \times B} = \frac{\partial}{\partial x} \langle v_{E \times B}^y \rangle$ . Sheared flows tend to squeeze and break the turbulent eddies, regulating the turbulence level and transferring energy to smaller

spatial scales.<sup>23</sup>

The quotient  $\omega_{E \times B} / \gamma_{\max}$  is shown in TABLE III for the mixed ITG-TEM cases. For ITG-1, ITG-2 and ITG-3 this quotient grows with the isotope mass. This is an indication that the higher the mass, the more efficient the turbulence regulation by sheared flows. This is coherent with the fact that  $\Delta_{HD} > \Delta_{DT}$  from TABLE I. Because  $\omega_{E \times B} / \gamma_{\max}$  increases more from H to D than from D to T, there is more transport regulation and thus more deviation in the H-D stage. On the other hand, the marginally unstable system does not exhibit this behavior because the quotient remains constant.

When dealing with TEM turbulence (FIG. 10), we observe that the growth rate does not have a maximum in the  $k_y$  range studied, due to the influence of the ETGs. For simplicity we choose the growth rate corresponding to the scale where the heat flux peaks ( $k_y \rho_s \sim 0.3$ ) to normalize  $\omega_{E \times B}$ . This results are shown in TABLE IV. The behavior of  $\omega_{E \times B} / \gamma_{\max}$  for TEMs reveals two main features. First, increasing  $\tau$  reduces  $\omega_{E \times B} / \gamma_{\max}$ , i.e., reduces the zonal flow activity.<sup>24</sup> Second,  $\omega_{E \times B} / \gamma_{\max}$  increases with the atomic mass. Thus, the turbulence regulation by zonal flows is increased and deviations from  $\sqrt{A}$  scaling are found in the heat fluxes. For  $\tau = 3$  the zonal flows are not so effective and we recover the gyro-Bohm scaling. Unfortunately, for these TEM simulations there is no evident relation between  $\Delta_{HD}$ ,  $\Delta_{DT}$  and  $\omega_{E \times B} / \gamma_{\max}$ .

Finally, we have used other GENE diagnostics to calculate the GAM intensity and the radial correlation length of the electric potential (size of the turbulent eddies). In the local

Label	$\omega_{E \times B} / \gamma_{\max}$		
	H	D	T
ITG-1	3.8	4.3	4.4
ITG-2	3.5	4.1	4.3
ITG-3	2.4	2.7	2.9
ITG-Marginal	6.1	6.0	6.1

TABLE III: Quotient between the zonal flow shear rate and the maximum linear growth rate for each isotope in the mixed ITG-TEM simulations. Except for the marginally unstable case, the quotient increases with the isotope mass.

Label	$\tau$	$\omega_{E \times B} / \gamma(k_y \rho_s = 0.3)$		
		H	D	T
TEM-1	1	2.9	3.3	3.4
	3	2.2	2.7	2.8
TEM-2	1	2.7	3.0	3.3
	3	2.1	2.6	2.7
TEM-3	1	3.1	3.5	3.6
	3	2.1	2.5	2.7
TEM-4	1	3.0	3.5	3.8
	3	2.4	2.8	2.9
TEM-5	1	3.0	3.4	3.6
	3	2.4	2.7	2.9

TABLE IV: Quotient between the zonal flow shear rate and the linear growth rate at  $k_y \rho_s = 0.3$  for each isotope in the TEM simulations. The quotient always increases with the isotope mass.

geometry used, none of them presented clear variations with the isotope mass.

## V. CONCLUSIONS

We have investigated the dependence of the heat flux on the ion mass using gyrokinetic simulations of turbulent transport. Based on previous linear works, in which the RH residual level exhibits mass dependence, we discovered that for some types of ITG/TEM and TEM turbulence an isotope effect is clearly visible. These cases mostly correspond to  $\tau = 1$ , whereas for  $\tau = 3$  the isotope effect is weaker or inexistent. We observe a typical reduction of  $\Delta_{HT} \approx -20\%$  in the total heat flux compared with classical gyro-Bohm scaling. This fact is connected to the intensity of the zonal flow regulation on the turbulence, characterized by the zonal  $E \times B$  shear rate. According to the results presented in this paper, the isotope mass would be expected to have impact on the confinement in tokamaks with TEM activity. Depending on the plasma gradients, different  $T_i$  and  $T_e$  can suppress the isotope effect. Hence, our simulations appear to be consistent with the isotope zonal flow dependence suggested by Hahm and, more-

over, the relation can be extended to the nonlinear regime.

The intensity of the isotope effect calculated here is smaller than the scaling observed in various experiments, where even absolute values of  $Q_D < Q_H$  have been measured. Other physical effects, like the inclusion of collisions, impurities, electromagnetic effects and more complex geometries like shaped tokamaks or stellarators are left for further work. Specially, edge physics and  $\rho^*$  effects are expected to be important, since the heat flux tends to reduce with it.<sup>25</sup>

## ACKNOWLEDGMENTS

The simulations presented in this work were carried out using the HELIOS supercomputer system at Computational Simulation Centre of International Fusion Energy Research Centre (IFERC-CSC), Aomori, Japan, and the HYDRA supercomputer at the Rechenzentrum Garching (RZG), Germany. This work has furthermore been carried out within the framework of the EUROfusion Consortium and has received funding from the European Union's Horizon 2020 research and innovation programme under grant agreement number 633053. The views and opinions expressed herein do not necessarily reflect those of the European Commission. The research leading to these results has also received funding from the European Research Council under the European Unions Seventh Framework Programme (FP7/2007V2013)/ERC Grant Agreement No. 277870.

<sup>1</sup>M. Bessenrodt-Weberpals, F. Wagner, O. Gehre, L. Giannone, J.V. Hoffmann, A. Kallenbach, K. McCormick, V. Mertens, H.D. Murmann, F. Rytter, B.D. Scott, G. Siller, F.X. Soldner, A. Stabler, K.-H. Steuer, U. Stroth, N. Tsois, H. Verbeek and H. Zohm. The isotope effect in ASDEX. *Nuclear Fusion*, **33**, 081205 (1993).

<sup>2</sup>Ulrich Stroth. A comparative study of transport in stellarators and tokamaks. *Plasma Physics and Controlled Fusion*, **40**, 01 (1998).

<sup>3</sup>F. Rytter, T. Puetterich, M. Reich, A. Scarabosio, E. Wolfrum, R. Fischer, M. Gemisic Adamov, N. Hicks, B. Kurzan, C. Maggi, R. Neu, V. Rohde, G. Tardini and the ASDEX Upgrade TEAM. H-mode threshold and confinement in helium and deuterium in ASDEX-Upgrade. *Nuclear Fusion*, **49**, 062003 (2009).

<sup>4</sup>R. J. Hawryluk, H. Adler, P. Alling, C. Ancher, H. Anderson, J. L. Anderson, D. Ashcroft, Cris W. Barnes, G. Barnes, S. Batha, M. G. Bell, R. Bell, M. Bitter, W. Blanchard, N. L. Bretz, R. Budny, C. E. Bush, R. Camp, M. Caorlin, S. Cauffman, Z. Chang, C. Z. Cheng, J. Collins, G. Coward, D. S. Darrow, J. DeLooper, H. Duong, L. Dudek, R. Durst, P. C. Efthimion, D. Ernst, R. Fisher, R. J. Fonck, E. Fredrickson, N. Fromm, G. Y. Fu, H. P. Furth, C. Gentile, N. Gorelenkov, B. Grek, L. R. Grisham, G. Hammett, G. R. Hanson, W. Heidbrink, H. W. Herrmann, K. W. Hill, J. Hosea, H. Hsuan, A. Janos, D. L. Jassby, F. C. Jobs, D. W. Johnson, L. C. Johnson, J. Kamperschroer, H. Kugel, N. T. Lam, P. H. LaMarche, M. J. Loughlin, B. LeBlanc, M. Leonard, F. M. Levinton, J. Machuzak, D. K. Mansfield, A. Martin, E. Mazzucato, R. Majeski, E. Marmor, J. McChesney, B. McCormack, D. C. McCune, K. M. McGuire, G. McKee, D. M. Meade, S. S. Medley, D. R. Mikkelsen, D. Mueller, M. Murakami, A. Nagy, R. Nazikian, R. Newman, T. Nishitani, M. Norris, T. O'Connor, M. Oldaker, M. Osakabe, D. K. Owens, H. Park, W. Park, S. F. Paul, G. Pearson, E. Perry, M. Petrov, C. K. Phillips, S. Pitcher, A. Ramsey, D. A. Rasmussen, M. H. Redi, D. Roberts, J. Rogers, R. Rossmassler, A. L. Roquemore, E. Ruskov, S. A. Sabbagh, M. Sasao, G. Schilling, J. Schivell, G. L. Schmidt, S. D. Scott, R. Sisingh, C. H. Skinner, J. Snipes, J. Stevens, T. Stevenson, B. C. Stratton, J. D. Strachan, E. Synakowski, W. Tang, G. Taylor, J. L. Terry, M. E. Thompson, M. Tuszewski, C. Vannoy, A. von Halle, S. von Goeler, D. Voorhees, R. T. Walters, R. Wieland, J. B. Wilgen, M. Williams, J. R.

- Wilson, K. L. Wong, G. A. Wurden, M. Yamada, K. M. Young, M. C. Zarnstorff and S. J. Zweben. Confinement and heating of a deuterium-tritium plasma. *Phys. Rev. Lett.*, **72**, 3530 (1994).
- <sup>5</sup>U. Stroth, B. Branas, T. Estrada, L. Giannone, H. J. Hartfuss, M. Hirsch, M. Kick, G. Kuehner, S. Sattler, J. Baldzuhn, R. Brakel, V. Erckmann, R. Jaenicke, H. Ringler, F. Wagner, the ECRH Group and the W7-AS Team. Recent transport experiments in W7-AS on the stellarator-tokamak comparison. *Physica Scripta*, **51**, 05655 (1995).
- <sup>6</sup>K. Tanaka, S. Okamura, M. Osakabe, T. Minami, K. Ida, Y. Yoshimura, M. Isobe, S. Morita and K. Matsuoka. Isotope effects on transport in compact helical system. In *Proc. of 41th European Physical Society Meeting on Cont. Fusion and Plasma Physics*, Berlin, Germany (2014).
- <sup>7</sup>F. Rytter, S.K. Rathgeber, L. Barrera Orte, M. Bernert, G.D. Conway, R. Fischer, T. Happel, B. Kurzan, R.M. McDermott, A. Scarabosio, W. Suttrop, E. Viezzer, M. Willensdorfer, E. Wolfrum and the ASDEX Upgrade Team. Survey of the H-mode power threshold and transition physics studies in ASDEX-Upgrade. *Nuclear Fusion*, **53**, 113003 (2013).
- <sup>8</sup>Y. Xu, C. Hidalgo, I. Shesterikov, A. Krämer-Flecken, S. Zoletnik, M. Van Schoor, M. Vergote and the TEXTOR Team. Isotope effect and multiscale physics in fusion plasmas. *Phys. Rev. Lett.*, **110**, 265005 (2013).
- <sup>9</sup>T.S. Hahm, Lu Wang, W.X. Wang, E.S. Yoon and F.X. Duthoit. Isotopic dependence of residual zonal flows. *Nuclear Fusion*, **53**, 072002, (2013).
- <sup>10</sup>A. M. Dimits, G. Bateman, M. A. Beer, B. I. Cohen, W. Dorland, G. W. Hammett, C. Kim, J. E. Kinsey, M. Kotschenreuther, A. H. Kritiz, L. L. Lao, J. Mandrekas, W. M. Nevins, S. E. Parker, A. J. Redd, D. E. Shumaker, R. Sydora and J. Weiland. Comparisons and physics basis of tokamak transport models and turbulence simulations. *Physics of Plasmas (1994-present)*, **7**, 03969 (2000).
- <sup>11</sup>F. Jenko, W. Dorland, M. Kotschenreuther and B. N. Rogers. Electron temperature gradient driven turbulence. *Physics of Plasmas (1994-present)*, **7**, 051904 (2000).
- <sup>12</sup>A. J. Brizard and T. S. Hahm. Foundations of nonlinear gyrokinetic theory. *Rev. Mod. Phys.*, **79**, 421 (2007).
- <sup>13</sup>url = <http://gene.rzg.mpg.de>
- <sup>14</sup>P. Morel, A. Banon-Navarro, M. Albrecht-Marc, D. Carati, F. Merz, T. Goerler, and F. Jenko. Gyrokinetic large eddy simulations. *Physics of Plasmas (1994-present)*, **18**, 072301 (2011).
- <sup>15</sup>A. Bañon Navarro, B. Teaca, F. Jenko, G. W. Hammett, T. Happel and ASDEX Upgrade Team. Applications of large eddy simulation methods to gyrokinetic turbulence. *Physics of Plasmas (1994-present)*, **21**, 032304 (2014).
- <sup>16</sup>M. N. Rosenbluth and F. L. Hinton. Poloidal flow driven by ion-temperature-gradient turbulence in tokamaks. *Phys. Rev. Lett.*, **80**, 724 (1998).
- <sup>17</sup>F. Merz and F. Jenko. Nonlinear saturation of trapped electron modes via perpendicular particle diffusion. *Phys. Rev. Lett.*, **100**, 035005 (2008).
- <sup>18</sup>D. R. Ernst, J. Lang, W. M. Nevins, M. Hoffman, Y. Chen, W. Dorland and S. Parker. Role of zonal flows in trapped electron mode turbulence through nonlinear gyrokinetic particle and continuum simulation. *Physics of Plasmas (1994-present)*, **16**, 055906 (2009).
- <sup>19</sup>X. Garbet, Y. Idomura, L. Villard and T.H. Watanabe. Gyrokinetic simulations of turbulent transport. *Nuclear Fusion*, **50**, 043002 (2010).
- <sup>20</sup>T. Goerler and F. Jenko. Scale separation between electron and ion thermal transport. *Phys. Rev. Lett.*, **100**, 185002 (2008).
- <sup>21</sup>F. Jenko, W. Dorland and G.W. Hammet. Critical gradient formula for toroidal electron temperature gradient modes. *Physics of Plasmas (1994-present)*, **8**, 094096 (2001).
- <sup>22</sup>I. Pusztai, J. Candy and P. Gohil. Isotope mass and charge effects in tokamak plasmas. *Physics of Plasmas (1994-present)*, **18**, 122501 (2011).
- <sup>23</sup>P. H. Diamond, S-I. Itoh, K. Itoh and T. S. Hahm. Zonal flows in plasma. A review. *Plasma Physics and Controlled Fusion*, **47**, 05-R35 (2005).
- <sup>24</sup>Tilman Dannert and Frank Jenko. Gyrokinetic simulation of collisionless trapped-electron mode turbulence. *Physics of Plasmas (1994-present)*, **12**, 072309 (2005).
- <sup>25</sup>B. F. McMillan, X. Lapillonne, S. Brunner, L. Villard, S. Jolliet, A. Bottino, T. Görler and F. Jenko. System size effects on gyrokinetic turbulence. *Phys. Rev. Lett.*, **105**, 155001 (2010).